Electronic Supplementary Material (ESI) for Dalton Transactions.

Supporting Information

Exploring the Structure Dependence of Metal-free Carbon Electrocatalysts on Zinc-based Metal-organic Framework Types

Wenfang Si,[a#] Qianjie Xie,[a#] Ruiyi Zhang,[a] Zheng Wang,*[b] Yehua Shen*[b] and Hiroshi Uyama

[a]Key Laboratory of Synthetic and Natural Functional Molecule Chemistry of Ministry of Education, College of Chemistry and Materials Science, Northwest University, No. 1, Xuefu Road, 710127 Xi'an, Shaanxi, China.

[b]College of Food Science and Engineering, Northwest University, No. 229 Taibai North Road, 710069 Xi'an, Shaanxi, China.

[c]Department of Applied Chemistry, Graduate School of Engineering, Osaka University, Suita 565-0871, Japan.

[#]These authors contributed equally.

Corresponding authors: Dr. Zheng Wang, zheng.wang@nwu.edu.cn; Prof. Yehua Shen, yhshen@nwu.edu.cn.

Experiment

1. Electrocatalysts synthesis

Synthesis of Zn_3BDT_3. The linker H_2BDT was prepared by referring *Ref.* [1], and Zn_3BDT_3 was prepared according to a reported method.[2] 1000 mg $Zn(NO_3)_2{\cdot}6H_2O$ and 350 mg H_2BDT were dissolved in 50 mL methanol and 50 mL DMF to prepare the solutions, respectively. The two solutions were mixed and allowed to stand in the open air until colorless, block-shaped crystals precipitated. Then the crystals were collected by filtration, washed with DMF and ether three times, and dried by vacuum at room temperature for 24 h.

Synthesis of MOF-5. MOF-5 was synthesized following a reported method.[3] 16.99 g $Zn(OAc)_2{\cdot}2H_2O$ was dissolved in 500 mL DMF, and 5.065 g terephthalic acid and 8.5 mL triethylamine were dissolved in 400 mL of DMF. The $Zn(OAc)_2$ solution was poured into the terephthalic acid solution under stirring. White precipitate was formed immediately, and the mixture was allowed to stir for overnight. The solid was collected by centrifugation at 9000 rpm for 10 min, and washed with DMF and methanol two times, then dried at 80 °C for overnight to obtain MOF-5.

Preparation of catalysts. The mixture of MOFs and urea (1 : 2 by weight) were pyrolyzed in a tube furnace at 1000 °C for 1 h under flowing to obtain the catalysts. The heating rate was set as 5 °C min^{-1}. Besides, the mass ratio of MOFs and urea (1 : 1 and 1 : 3) were tuned to derive other carbon catalysts for comparison. The temperature and dwelling time used in our previous work[4] was adopted herein.

2. Catalysts characterization

Electrocatalyst characterization. The single crystal data of Zn_3BDT_3 were collected on a Bruker SMART APEX II CCD diffractometer using monochromatic Mo Kα radiation (λ = 0.71073 Å) at 293K. The X-ray diffraction (XRD) on MOFs and derived carbons were recorded on a Bruker D8 ADVANCE (equipped with Cu Kα radiation, λ = 1.5406 Å) in the 2θ range of 5–80°. X-ray photoelectron spectroscopy (XPS) measurements on derived carbons were done on a PHI 5000 Versaprode III spectrometer. Fourier transform infrared (FT-IR) spectra of MOFs were generated on a Bruker INVENIO R FT-IR spectrometric analyzer equipping ATR. Thermogravimetric analysis (TGA) was conducted in the range of 30–800 °C under N_2 flow on a NETZSCH instrument STA 449C. Raman spectra of derived carbon catalysts were generated on a LABRAM.HR dispersive Raman spectrometer using 532 nm laser as the excitation source. The morphology of the MOFs and derived carbons were detected by scanning electron microscopy (SEM, HITACHI SU3500, Japan) and transmission electron microscopy (TEM, FEI Talos F200X, USA). Besides, energy-dispersive X-ray spectroscopy (EDS) elemental mapping of C, N and O were also studied on the TEM instrument. The porosity and surface area of carbon catalysts were acquired from N_2 adsorption/desorption isotherms recorded on a Micromeritics 3flex instrument at 77 K. The pore size distributions were analyzed by the Barrett−Joyner−Halenda (BJH) method. Elemental composition of derived carbons were confirmed on a VarioEL III instrument.

ORR tests. A CHI 760E electrochemical analyzer (CH Instruments, Inc., Shanghai) together with a rotating ring-disc electrode (RRDE) from Princeton Instruments (Model: 636A) were employed to perform the electrochemical measurements. All measurements were done in a

standard three electrodes system employing Ag/AgCl (saturated KCl) and platinum wire as the electrode and counter electrode, respectively. 2 mg catalyst homogeneously dispersed in water/ethanol mixed solvent (1 mL, v/v = 1 : 9) containing 10 μL of 5 wt% Nafion solution was prepared, then 25 μL of the catalyst ink was dripped on a glassy carbon (GCE, 5.0 mm diameter) to prepared the working electrode. The catalyst loading amount was estimated ~0.25 mg cm^{-2}. Cyclic voltammetry (CV) curves were recorded in the O_2- and N_2-saturated 0.1 M KOH solution for comparison, respectively. Linear-sweep voltammetry (LSV) curves were measured in the O_2-saturated 0.1 M KOH solution at different rotating rate (400–2025 rpm) All the measurements were done with a scan rate of 5 mV s^{-1}. In this work, all reported potentials have been converted to that of RHE.

The electron transferred numbers (n) and the kinetic current densities (J_K) were calculated by the Koutecký–Levich (K-L) equation according to the LSV curves at different rotating rate. Herein, the K-L is $1/J = 1/J_K + 1/(B\omega^{1/2})$, where J and J_k are the measured current density and the kinetic current density respectively, ω is the electrode rotating rate. B is determined from the Levich slope $B = 0.2\, n\, F\, C_0\, D_0^{2/3}\, v^{-1/6}$. Herein, F is the Faraday constant (96485 C mol^{-1}). C_0, D_0 and v are the O_2 concentration, O_2 diffusion coefficient in the 0.1 M KOH solution and kinematics viscosity of electrolyte solution, of which the values are1.2×10^{-6} mol cm^{-3}, 1.9×10^{-5} cm^2 s^{-1} and 0.01 cm^2 s^{-1}, respectively. The constant 0.2 is adopted when rotating speed is expressed in rpm.

The rotating ring-disc electrode (RRDE) measurements were performed to determine the electron transfer number (n) and H_2O_2 yield (H_2O_2%). The values were calculated by the below equations:

$$H_2O_2\% = 200 \times \frac{I_r/N}{I_d + I_r/N}$$

$$n = 4 \times \frac{I_d}{I_d + I_r/N}$$

where I_d and I_r are the disk current and ring current, respextively, and N is the current collection efficiency of the Pt ring (0.37).

Zn–air battery. The ZABs were assembled employing N1OC or N3OC catalyst loaded carbon paper as the air-cathode, polished zinc plate (thickness: 0.5 mm) as the anode and 6 M KOH solution containing 0.2 M $Zn(OAc)_2$ as the alkaline electrolyte. The catalyst loading was about 1 mg cm^{-2}. For comparison, Pt/C-based ZAB were also built in a similar way. The battery measurements were done at room temperature. Cycling test was performed by discharging for 5 min and then charging for 5 min of min at j = 5 mA cm^{-2}.

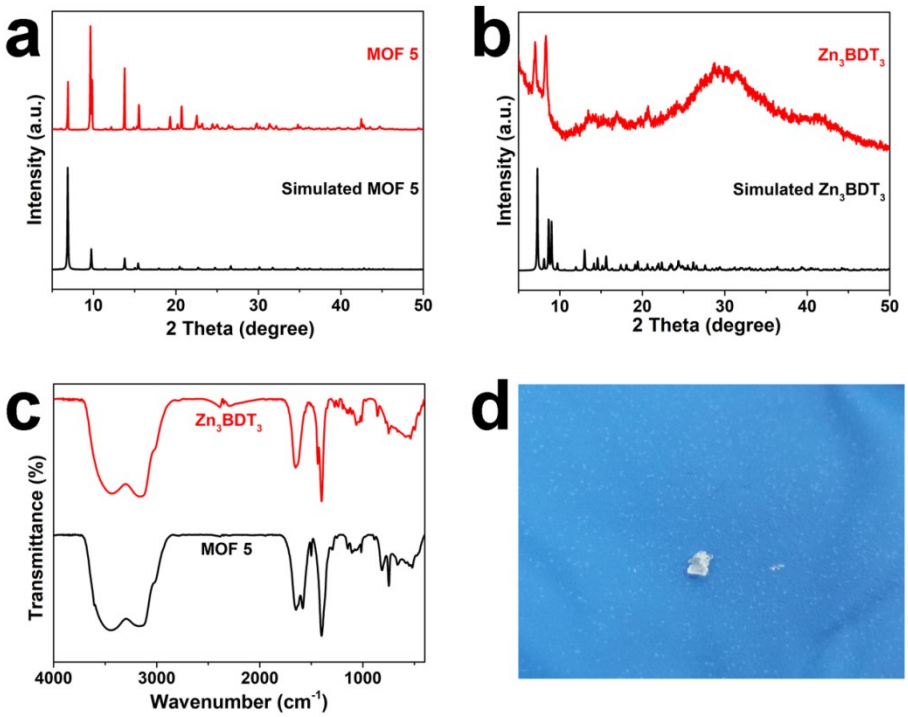

Figure S1. (a) The X-ray diffraction (XRD) patterns of (a) MOF-5 and (b) Zn_3BDT_3, (c) Fourier transformation infrared (FT-IR) spectra of MOF-5 and Zn_3BDT_3, and (d) Photograph of of Zn_3BDT_3 crystal.

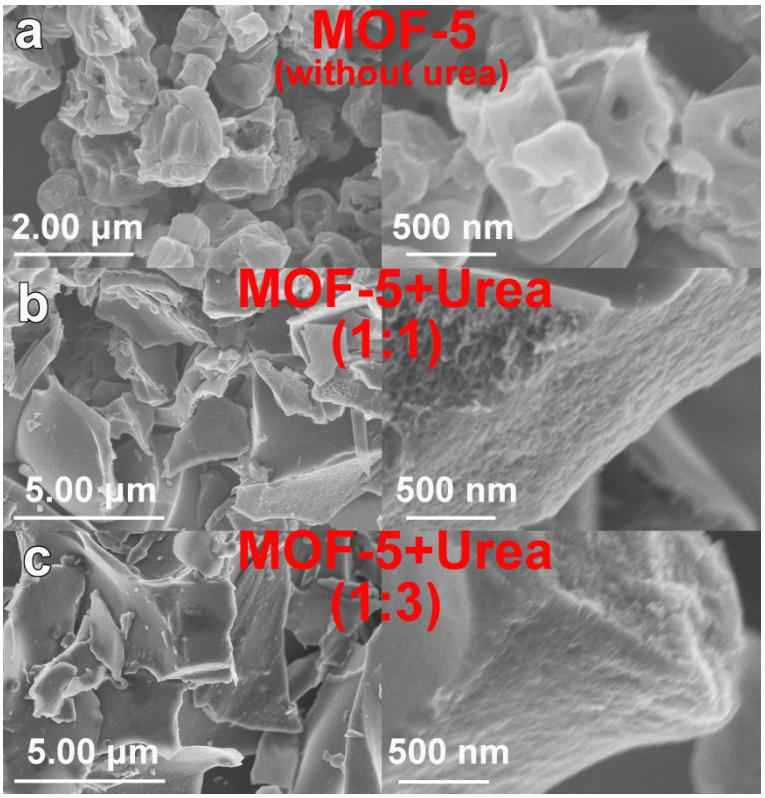

Figure S2. The SEM images of MOF-5 derived carbon catalysts with different urea dosage.

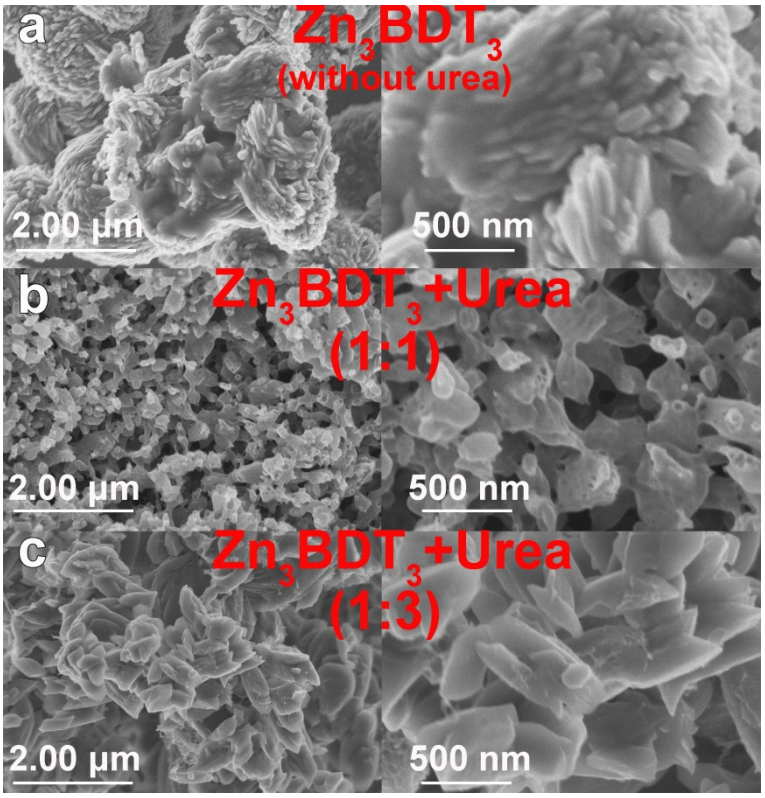

Figure S3. The SEM images of Zn_3BDT_3 derived carbon catalysts with different urea dosage.

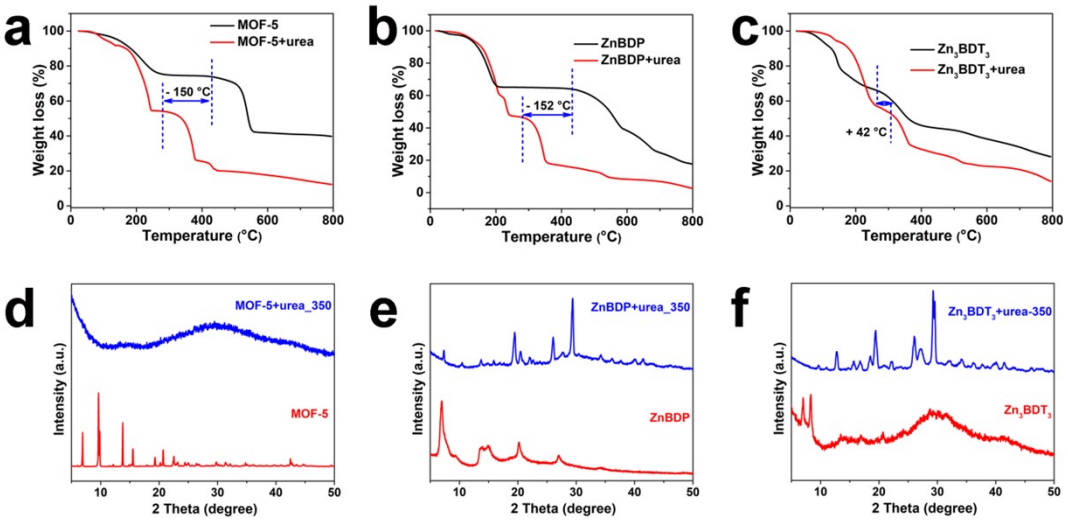

Figure S4. The (a—c) thermogravimetric analysis (TGA) curves and (d—f) XRD patterns of fresh MOF precursors and their residues after heated to 350 °C with urea.

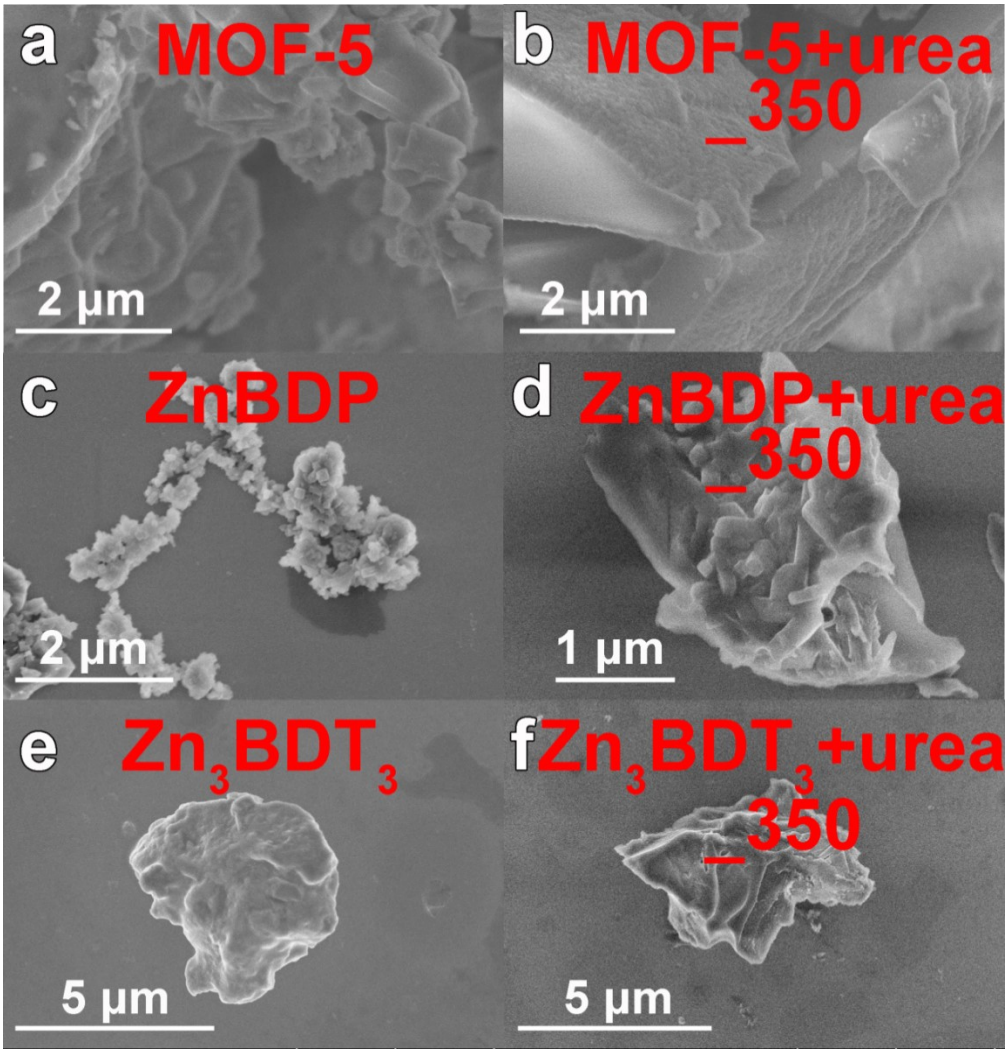

Figure S5. The scanning electron microscopy (SEM) images of fresh MOF precursors and their residues after heated to 350 °C with urea.

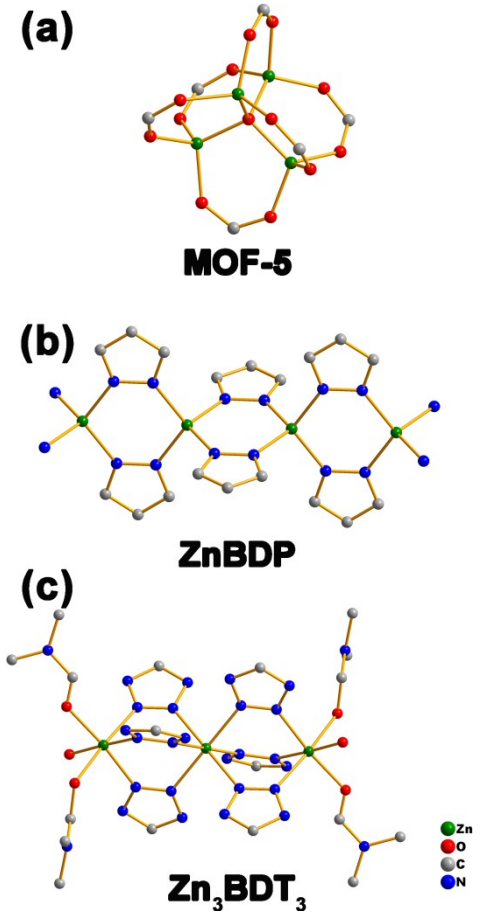

Figure S6. The coordination environment of Zn nodes of (a) MOF-5, (b) ZnBDP, and (c) Zn_3BDT_3.

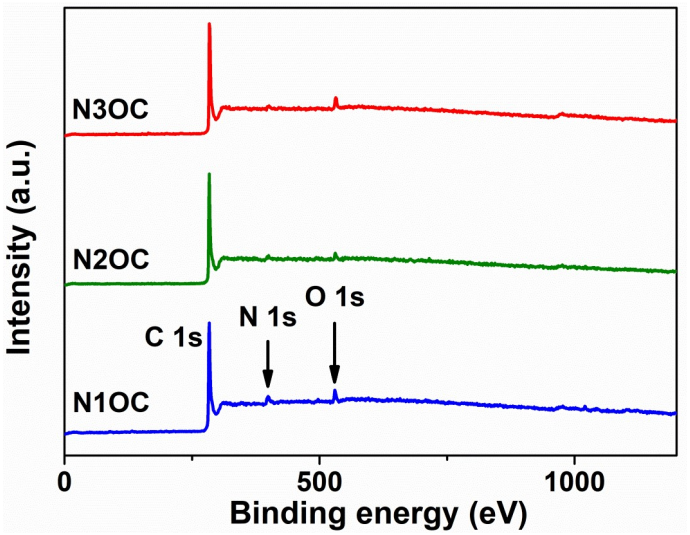

Figure S7. The full XPS spectra of N1OC, N2OC and N3OC.

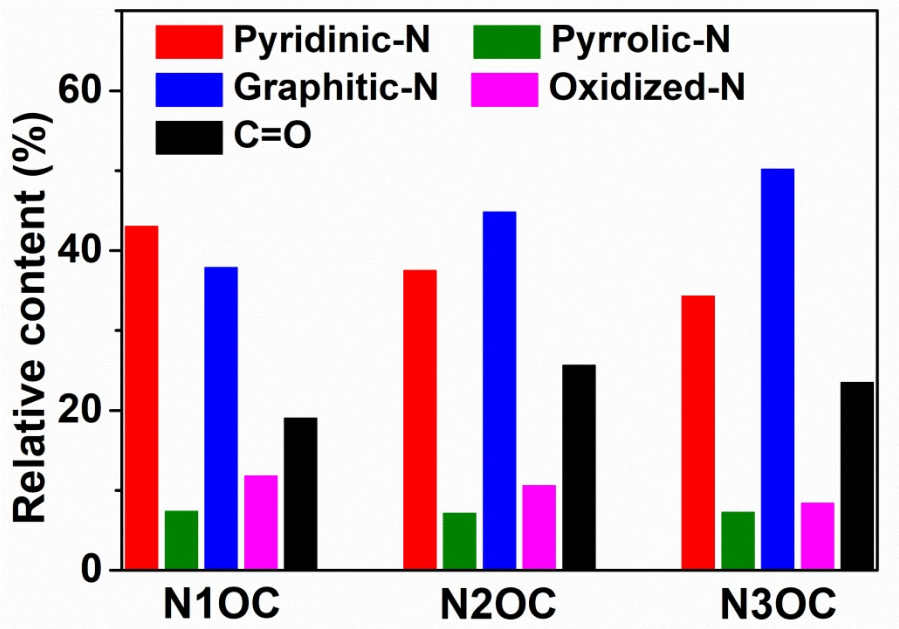

Figure S8. The relative content of pyridinic N, pyrrolic N, graphitic N, oxidized N and C=O species of N1OC, N2OC and N3OC.

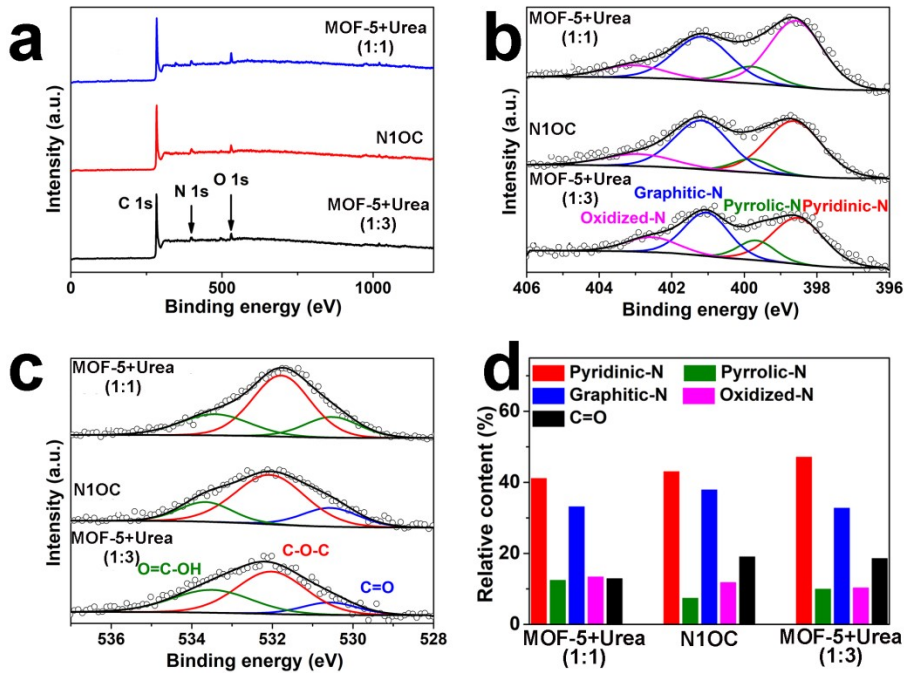

Figure S9. (a) the full XPS spectra, (b) N 1s and (c) O 1s XPS spectra and (d) the relative contents of pyridinic N, pyrrolic N, graphitic N, oxidized N and C=O species of MOF-5 derived carbon materials with different urea dosage.

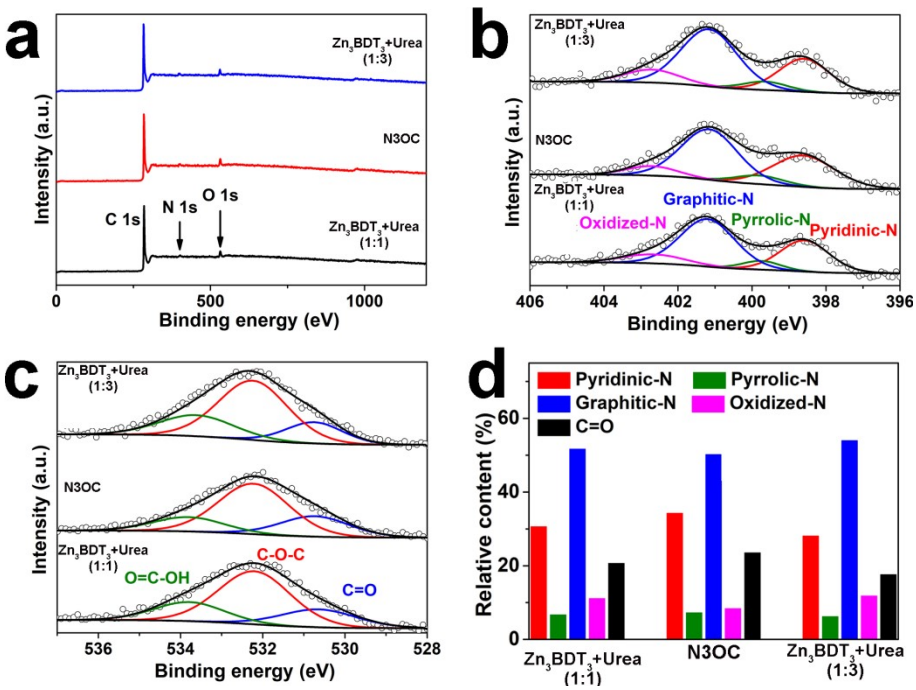

Figure S10. (a) the full XPS spectra, (b) N 1s and (c) O 1s XPS spectra and (d) the relative contents of pyridinic N, pyrrolic N, graphitic N, oxidized N and C=O species of Zn_3BDT_3 derived carbon materials with different urea dosage.

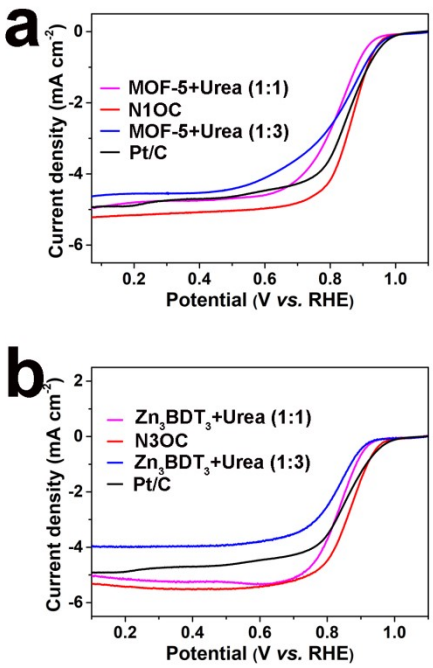

Figure S11. The linear-sweep voltammetry (LSV) curves of (a) MOF-5 and (b) Zn_3BDT_3 derived carbons with different urea dosage in an O_2-saturated 0.1 M of KOH solution at 5 mV s^{-1} with 1600 rpm.

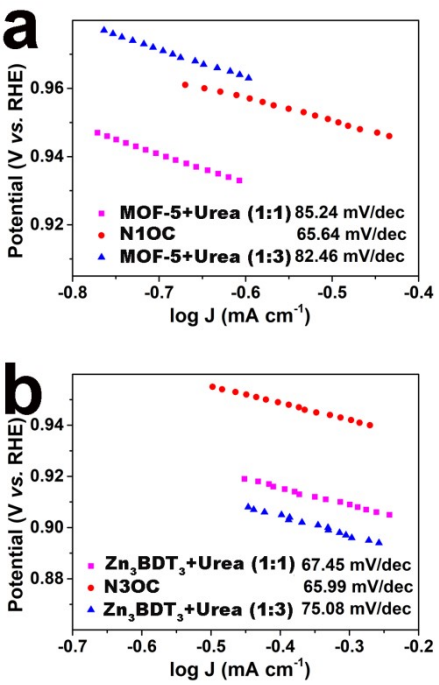

Figure S12. The Tafel slope of (a) MOF-5 and (b) Zn_3BDT_3 derived carbons with different urea dosage.

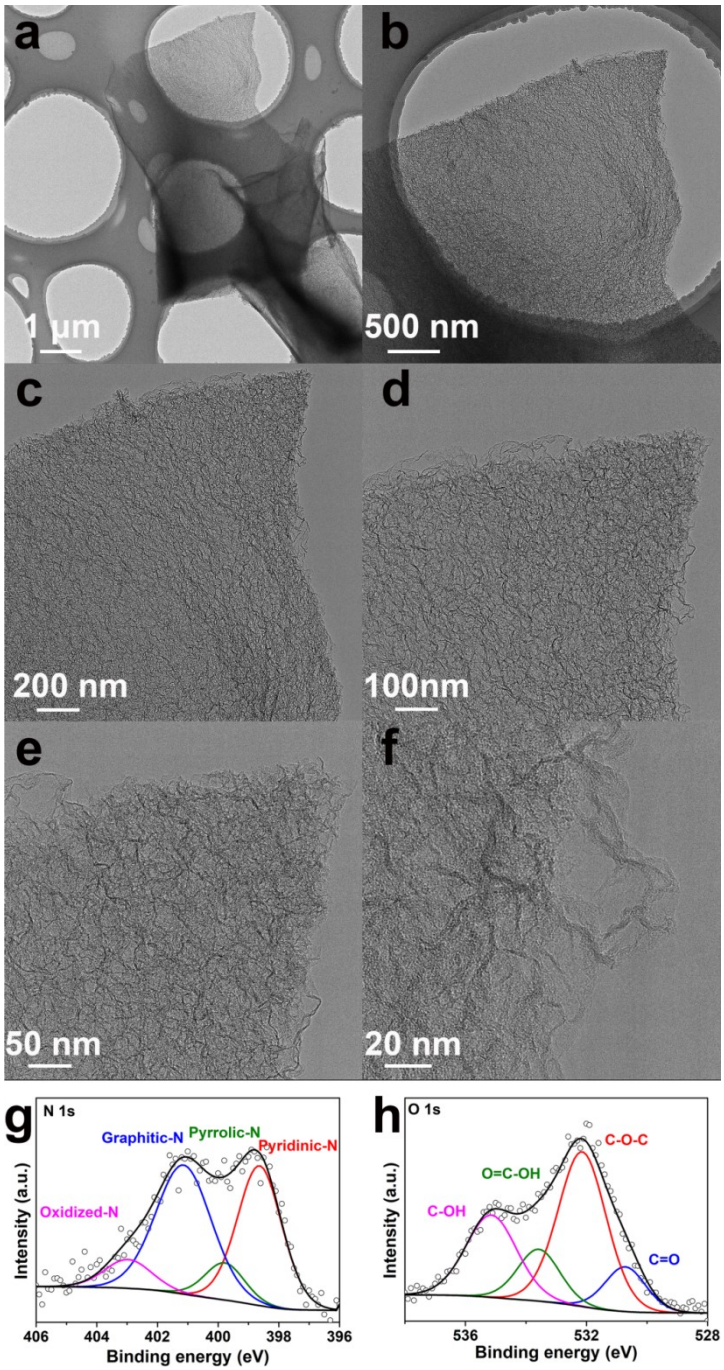

Figure S13. (a-f) The TEM images, (g) N 1s and (h) O 1s XPS spectra of N1OC after stability test.

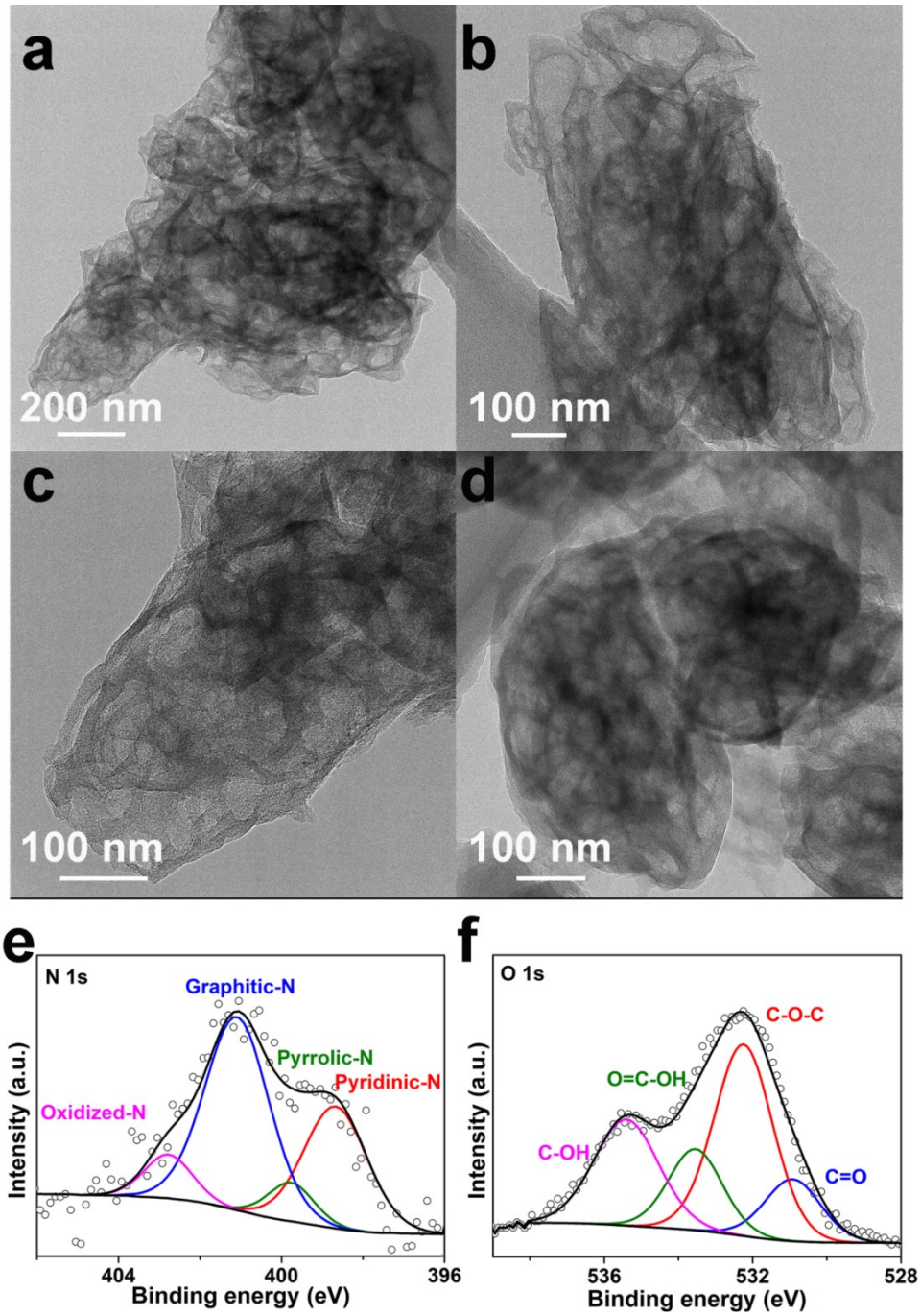

Figure S14. (a-d) The TEM images, (e) N 1s and (f) O 1s XPS spectra of N3OC after stability test.

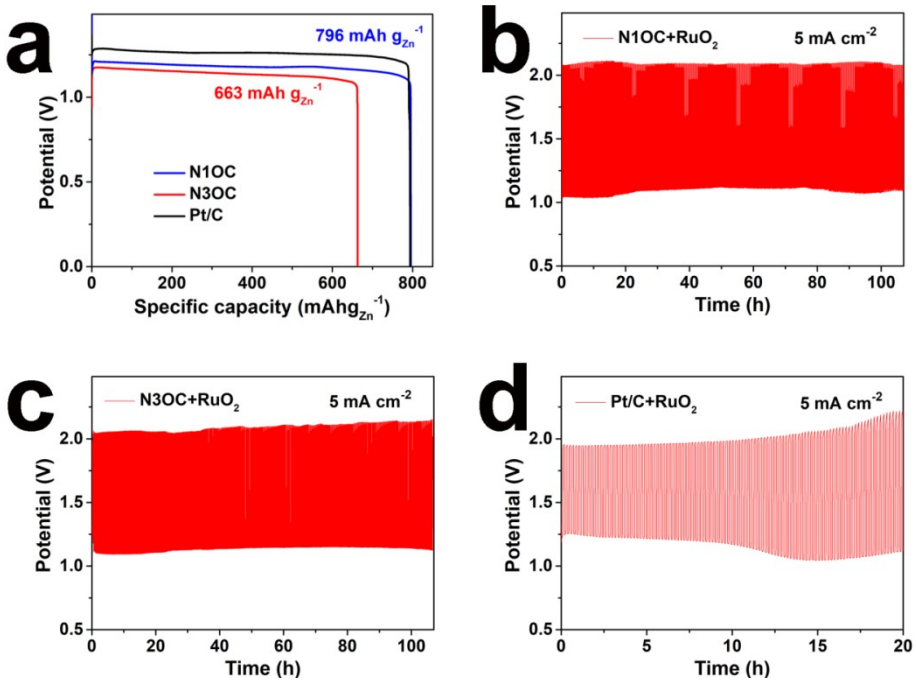

Figure S15. (a) The specific capacities of N1OC, N3OC and Pt/C based batteries; the cycling performance of rechargeable Zn-air batteries with (b) N1OC + RuO_2 mixture, (c) N3OC + RuO_2 mixture and (d) Pt/C + RuO_2 mixture as air cathodes at the current density of 5 mA cm^{-2}.

Table S1. The elemental analysis of N1OC, N2OC and N3OC (wt%).

Content	C	N	H	O
N1OC	71.72	7.95	1.41	18.92
N2OC	75.10	4.46	2.00	18.44
N3OC	73.93	4.49	2.03	19.55

Table S2. The relative content (%) of pyridinic N, pyrrolic N, graphitic N and oxidized N in N1OC, N2OC and N3OC.

Content	Pyridinic N	Pyrrolic N	Graphitic N	Oxidized N	Pyridinic N + Graphitic N
N1OC	42.99	7.37	37.85	11.79	80.84
N2OC	37.49	7.13	44.81	10.57	82.30
N3OC	34.26	7.22	50.15	8.37	84.41

Table S3. The relative content of pyridinic N, pyrrolic N, graphitic N and oxidized N of MOF-5 derived catalysts prepared with different urea dosage.

Content	Pyridinic N	Pyrrolic N	Graphitic N	Oxidized N	Pyridinic N + Graphitic N
MOF-5+Urea (1 : 1)	41.09	12.43	33.13	13.35	74.22
N1OC	42.99	7.37	37.85	11.79	80.84
MOF-5+Urea (1 : 3)	47.07	9.92	32.74	10.27	79.81

Table S4. The relative content of pyridinic N, pyrrolic N, graphitic N and oxidized N of Zn_3BDT_3 derived catalysts prepared with different urea dosage.

Content	Pyridinic N	Pyrrolic N	Graphitic N	Oxidized N	Pyridinic N + Graphitic N
Zn_3BDT_3+Urea (1 : 1)	30.59	6.67	51.64	11.10	82.23
N3OC	34.26	7.22	50.15	8.37	84.41
Zn_3BDT_3+Urea (1 : 3)	28.05	6.18	53.96	11.81	82.01

Table S5. The comparison of the ORR activity and ZAB performance of N1OC, N2OC and N3OC with other reported MOF-derived metal-free carbon catalysts.

Catalyst	Precursor	Heteroatom	ORR $E_{1/2}$ (V vs.RHE)	Open-circuit voltage (V)	Power density (mW cm^{-2})	Durability	Ref.
N1OC	MOF-5 and urea	N, O	0.873	1.55	109.58	107 h / 640 cycles	This work
N2OC	ZnBDP and urea	N, O	0.867	1.63	140.55	180h/1080 cycles	This work
N3OC	ZnBDT and urea	N, O	0.875	1.63	143.21	107 h / 640 cycles	This work
NC-D-NH_3	ZIF-7 and NH_3	N	0.82	/	/	/	5
A-Z-1000	ZIF-8 and amino acid	N	0.87 (E_{onset})	/	/	/	6
Z8&NaCl1:1-950	ZIF-8 and NaCl	N	0.85	1.51	89	/	7
GNHCNs_Urea	ZIF-8 and GO	N	0.86	/	126	95 h	8
NC-800	ZIF-8 and ZnO	N	0.85	/	/	/	9
O,N-graphene	Zn-BTC	N, O	0.842	1.43	152.8	160h	10
HPC(MV-c-PN)	ZIF-8, SiO_2 and g-C_3N_4	N	0.855	/	80.1	/	11
NHCP-1000	ZIF-8 and NaCl	N	0.86	1.44	272	160	12
NFPC-1100	COF-F	N, F	0.85	/	157	200 cycles	13
NCR1000	1,4-phenylenediurea	N	0.826	/	/	/	14
NCF	ZIF-8	N	0.85	1.41	173	/	15
h-N-CFs-800	3,5-diaminobenzoic and acid-1,3,5-benzenetricarboxaldehyde	N	0.87	/	/	/	16
F-N-AC-1000	N-based activated carbon	N, F	0.89	/	/	/	17

Reference

1. A. Maspero, S. Galli, N. Masciocchi and G. Palmisano, *Chem. Lett.*, 2008, 37, 956.
2. M. Dincă, A. F. Yu and J. R. Long, *J. Am. Chem. Soc.*, 2006, 128, 8904.
3. D. J. Tranchemontagne, J. R. Hunt and O. M. Yaghi, *Tetrahedron*, 2008, 64, 8553.
4. Q. Xie, W. Si, Y. Shen, Z. Wang and H. Uyama, *Nanoscale*, 2021, 13, 16296.
5. Q. Wu, J. Liang, J. D. Yi, D. L. Meng, P. C. Shi, Y. B. Huang and R. Cao, *Dalton Trans.*, 2019, 48, 7211.
6. G. Huang, M. Ren, Y. Wang, J. Zhou and J. Cai, *Mater. Chem. Phys.*, 2019, 237, 121856.
7. Y. Cao, Z. Liu, Y. Tang, C. Huang, Z. Wang, F. Liu, Y. Wen, B. Shan and R. Chen, *Carbon*, 2021, 180, 1.
8. X. Lu, L. Ge, P. Yang, O. Levin, V. Kondratiev, Z. Qu, L. Liu, J. Zhang and M. An, *Appl. Surface Sci.*, 2021, 562, 150114.
9. J. Meng, Z. Liu, X. Liu, W. Yang, L. Wang, Y. Li, Y.-C. Cao, X. Zhang and L. Mai, *J. Mater. Sci. Technol.*, 2021, 66, 186.
10. R. Song, X. Cao, J. Xu, X. Zhou, X. Wang, N. Yuan and J. Ding, *Nanoscale*, 2021, 13, 6174.
11. Z. Duan, G. Han, H. Huo, Z. Lin, L. Ge, C. Du, Y. Gao and G. Yin, *ACS Sustain. Chem. Eng.*, 2021, 9, 1264.
12. J. Yan, X. Zheng, C. Wei, Z. Sun, K. Zeng, L. Shen, J. Sun, M. H. Rümmeli and R. Yang, *Carbon*, 2021, 171, 320.
13. Y.-N. Sun, J. Yang, X. Ding, W. Ji, A. Jaworski, N. Hedin and B.-H. Han, *Appl.Catal. B: Environ.*, 2021, 297, 120448.
14. Q. Lai, H. Zheng, Z. Tang, D. Bi, N. Chen, X. Liu, J. Zheng and Y. Liang, *ACS Appl. Mater. Interfaces*, 2021, 13, 61129.
15. L. Zhang, T. Gu, K. Lu, L. Zhou, D.-S. Li and R. Wang, *Adv. Funct. Mater.*, 2021, 31, 2103187.
16. S. Li, Y. Wang, Y. Ding, Y. He, Y. Zhang, S. Li, J. Zhang and Y. Chen, *Chem. Eng. J.*, 2022, 430, 132969.
17. F. Zhang, D. Zhang, W. Liu, X. Li and Q. Chen, *Carbon*, 2022, 187, 67.